Mon. Not. R. Astron. Soc. **000**, 1–13 (2003) Printed 2 February 2008 (MN LATEX style file v2.2)

Cosmological parameter estimation using Very Small Array data out to $\ell = 1500$

Rafael Rebolo[1*], Richard A. Battye[2†], Pedro Carreira[2], Kieran Cleary[2], Rod D. Davies[2], Richard J. Davis[2], Clive Dickinson[2], Ricardo Genova-Santos[1], Keith Grainge[3], Carlos M. Gutiérrez[1], Yaser A. Hafez[2], Michael P. Hobson[3], Michael E. Jones[3], Rüdiger Kneissl[3], Katy Lancaster[3], Anthony Lasenby[3], J. P. Leahy[2], Klaus Maisinger[3], Guy G. Pooley[3], Nutan Rajguru[3], José Alberto Rubiño-Martin[1,4], Richard D.E. Saunders[3], Richard S. Savage[3‡], Anna Scaife[3], Paul F. Scott[3], Anže Slosar[3§], Pedro Sosa Molina[1], Angela C. Taylor[3], David Titterington[3], Elizabeth Waldram[3], Robert A. Watson[2¶], Althea Wilkinson[2]

[1] *Instituto de Astrofísica de Canarias, 38200 La Laguna, Tenerife, Spain.*
[2] *University of Manchester, Jodrell Bank Observatory, UK.*
[3] *Astrophysics Group, Cavendish Laboratory, University of Cambridge, UK.*
[4] *Present address: Max-Planck Institut für Asrtrophysik, Karl-Schwarzchild-Str. 1, Postfach 1317, 85741, Garching, Germany.*
[‡] *Present address: Astronomy Centre, University of Sussex, UK.*
[§] *Present address: Faculty of Mathematics & Physics, University of Ljubljana, 1000 Ljubljana, Slovenia.*
[¶] *Present address: Instituto de Astrofísica de Canarias, 38200 La Laguna, Tenerife, Spain.*
[*] *Email: rll@ll.iac.es*
[†] *Email: rbattye@jb.man.ac.uk*

Accepted —; received —; in original form 2 February 2008

ABSTRACT

We estimate cosmological parameters using data obtained by the Very Small Array (VSA) in its extended configuration, in conjunction with a variety of other CMB data and external priors. Within the flat ΛCDM model, we find that the inclusion of high resolution data from the VSA modifies the limits on the cosmological parameters as compared to those suggested by WMAP alone, while still remaining compatible with their estimates. We find that $\Omega_{\rm b}h^2 = 0.0234^{+0.0012}_{-0.0014}$, $\Omega_{\rm dm}h^2 = 0.111^{+0.014}_{-0.016}$, $h = 0.73^{+0.09}_{-0.05}$, $n_{\rm S} = 0.97^{+0.06}_{-0.03}$, $10^{10}A_{\rm S} = 23^{+7}_{-3}$ and $\tau = 0.14^{+0.14}_{-0.07}$ for WMAP and VSA when no external prior is included.On extending the model to include a running spectral index of density fluctuations, we find that the inclusion of VSA data leads to a negative running at a level of more than 95% confidence ($n_{\rm run} = -0.069 \pm 0.032$), something which is not significantly changed by the inclusion of a stringent prior on the Hubble constant. Inclusion of prior information from the 2dF galaxy redshift survey reduces the significance of the result by constraining the value of $\Omega_{\rm m}$. We discuss the veracity of this result in the context of various systematic effects and also a broken spectral index model. We also constrain the fraction of neutrinos and find that $f_\nu < 0.087$ at 95% confidence which corresponds to $m_\nu < 0.32$eV when all neutrino masses are the equal. Finally, we consider the global best fit within a general cosmological model with 12 parameters and find consistency with other analyses available in the literature. The evidence for $n_{\rm run} < 0$ is only marginal within this model.

Key words: cosmology: observations – cosmic microwave background

1 INTRODUCTION

Recent measurements of the cosmic microwave background (CMB) anisotropies have allowed the determination of a

large number of cosmological parameters with unprecedented accuracy. The Wilkinson Microwave Anisotropy Probe (WMAP) and pre-WMAP data sets can be fitted by a six-parameter ΛCDM model (see, for example, Bennett et al. 2003, Slosar et al. 2003). In order to break the degeneracies inherent in the CMB power spectrum (Efstathiou & Bond 1999), various authors have augmented measurements of the CMB with observations of large-scale structure (LSS), for example, the 2dF galaxy power spectrum (Percival et al. 2001, Percival et al. 2002), Lyman-α forest (Mandelbaum et al. 2003; Seljak et al. 2003), SDSS three-dimensional power spectrum (Tegmark et al. 2003), measurements of cosmic shear (Hoekstra et al. 2002) and the galaxy cluster luminosity function (Allen et al. 2003a), and/or information on the expansion rate of the Universe from measurements of the Hubble constant (Freedman et al. 2001) and high redshift supernovae (Perlmutter et al. 1999; Reiss et al. 1998).

High-resolution ($\ell \geqslant 700$) observations of CMB anisotropies provided by previously released data obtained by the Very Small Array (VSA, Grainge et al. 2003), the Arcminute Bolometer Array (ACBAR, Kuo et al. 2004) and the Cosmic Background Imager (CBI, Pearson et al. 2003), can also be important in reducing the impact of degeneracies and provide information on the parameters relating to the power spectrum of initial density fluctuations over a much wider range of scales. In particular, the WMAP team made use of these data in their analyses in order to improve the significance of their results (Spergel et al. 2003).

In this paper, we study the cosmological implications of the new CMB power spectrum measured by the VSA which has a good signal-to-noise ratio out to a multipole of $\ell = 1500$ (Dickinson et al. 2004). These observations cover 33 fields, as opposed to 9 in Grainge et al. (2003), representing an improvement of ~ 2 in signal-to-noise over the previous data. By virtue of the accurately measured temperature of Jupiter by WMAP, the absolute calibration uncertainty for these data is reduced to 3% on the power spectrum; something which will be significant in our subsequent discussion. The power spectrum is measured between $\ell = 300$ and $\ell = 1500$ with a resolution in ℓ-space of $\Delta\ell \approx 60$. Previous measurements of the power spectrum between $\ell = 130$ and $\ell = 900$ using the VSA compact configuration can be found in Scott et al. (2003).

We will first consider the standard six-parameter flat ΛCDM model, and then include extra parameters broadly in keeping with the approach taken in the papers published by the WMAP team (Spergel et al. 2003, Verde et al. 2003, Peiris et al. 2003). Our main focus will be on the initial spectrum of fluctuations, quantified by the running of the spectral index, which appears to be particularly sensitive to high-resolution data such as ours. In the case where we do not impose external priors on the CMB data (WMAP+VSA), we find that there is significant evidence ($> 2\sigma$) for negative running; something which is not implied by the WMAP data alone. The significance of this result is sensitive to the inclusion of external priors, the relative calibration of WMAP and VSA, and possible source/cluster contamination of the measured power spectrum, illustrating issues which are of great relevance in the era of precision cosmology. The result, if true, would be a significant challenge to models of slow-roll inflation, and so we also consider a broken spectral index model. As a final point, we consider a 12-parameter model fit to WMAP, WMAP+VSA and all available CMB data beyond $\ell > 1000$, illustrating the effects of external priors on the estimated parameters. Our results within this model are compatible with previous determinations, both by the WMAP team and others.

2 METHODOLOGY

2.1 Cosmological model

We will define the ΛCDM model as follows. First, we will assume that the Universe is flat and dominated by cold dark matter (CDM), baryons and a cosmological constant, Λ. The densities of these components relative to critical are denoted $\Omega_{\rm dm}$, $\Omega_{\rm b}$ and Ω_Λ respectively and we define $\Omega_{\rm m} = \Omega_{\rm dm} + \Omega_{\rm b}$ to be the overall matter density (CDM and baryons) in the same units. The expansion rate is quantified in terms of the Hubble constant $H_0 = 100h\,{\rm km\,sec^{-1}\,Mpc^{-1}}$ and we allow for instantaneous reionization at some epoch $z_{\rm re}(< 30)$ which can also be quantified in terms of an optical depth τ. The so-called physical densities of the CDM and baryons are defined as $\omega_{\rm dm} = \Omega_{\rm dm}h^2$ and $\omega_{\rm b} = \Omega_{\rm b}h^2$. We will consider only adiabatic models and, guided by the predictions of slow-roll inflation, we parameterize the initial fluctuation spectrum of this model by

$$P(k) = A_{\rm S}\left(\frac{k}{k_{\rm c}}\right)^{n_{\rm S}}\,, \qquad (1)$$

where $k_{\rm c} = 0.05{\rm Mpc}^{-1}$ is the arbitrarily chosen pivot point of the spectrum, $n_{\rm S}$ is the spectral index and $A_{\rm S}$ is the scalar power spectrum normalization.

We will modify this model by the inclusion of two other parameterizations of the power spectrum. We will, for the most part, consider a model with a running spectral index,

$$P(k) = A_{\rm S}\left(\frac{k}{k_{\rm c}}\right)^{n_{\rm S}+\frac{1}{2}n_{\rm run}\log(k/k_{\rm c})}\,, \qquad (2)$$

so that the overall spectral index of fluctuations is a function of scale, $n_{\rm S}(k)$, given by

$$n_{\rm S}(k) = \frac{d(\log\,P)}{d(\log\,k)} == n_{\rm S} + n_{\rm run}\log\left(\frac{k}{k_{\rm c}}\right)\,, \qquad (3)$$

where $n_{\rm run}$ is known as the running of the spectral index. For slow roll inflation to be well defined, one requires that $|n_{\rm run}| \ll |1 - n_{\rm S}|/2$ (Leach and Liddle, 2003). Under certain choices of priors we find that there is some evidence that this inequality is violated by the preferred fits to the data. We therefore consider an alternative model, which could be motivated by broken-scale invariance models of inflation (see, for example, Barriga et al. 2001), but is probably best thought of as a test of whether or not the data prefer a single power-law. The specific choice we will make is to consider

$$n(k) = n_1 \text{ for } k < k_{\rm c} \text{ and } n(k) = n_2 \text{ for } k > k_{\rm c}\,, \qquad (4)$$

with an appropriate normalization for $k > k_{\rm c}$ so as to make the power spectrum continuous and the same value of $k_{\rm c}$ as used in the standard ΛCDM model.

In our discussion of systematic effects in section 4, we will consider the possibility of an extra component to the anisotropies with $C_\ell = 2\pi A_{\rm X} \times 10^{-6}$. Such a component is motivated by foreground effects due to point sources and the

Sunyaev-Zel'dovich (SZ) effect from galaxy clusters along the line of sight. The temperature anisotropies due to such a component will be $(\Delta T_\ell)^2 = (\ell(\ell+1)C_\ell/(2\pi)) = A_{\rm X}\ell^2$ and could be significant for $\ell > 1000$. The VSA has a sophisticated procedure to extract the effects of point sources using a dedicated, co-located, single-baseline interferometer (see Dickinson et al. (2004) for details), and the VSA fields have been chosen to avoid very luminous X-ray clusters. There could still, however, be some residual contamination. Moreover, claims have been made of an excess signal between $\ell = 2000$ and $\ell = 4000$ by the CBI team (Mason et al. 2003), who attribute this to the SZ effect. If the signal is a large as is claimed, then it could be a contaminant even at lower ℓ. By including such a component in the parameter fitting, it should be possible to constrain the contribution at $\ell > 2000$ as well as gaining some insights into the possible systematic effects of making such an error.

The other parameters which we will consider in our analyses are: $f_\nu = \Omega_\nu/\Omega_{\rm dm}$, the fraction of the dark matter which is massive neutrinos; $\Omega_{\rm k} = 1 - \Omega_{\rm tot}$ ($\Omega_{\rm tot} = \Omega_{\rm dm} + \Omega_{\rm b} + \Omega_\nu + \Omega_\Lambda$), the curvature in units of the critical density; $w = P_{\rm Q}/\rho_{\rm Q}$, the equation-of-state parameter for a dark energy component modelled as a slowly rolling scalar field; $n_{\rm T}$ the spectral index of tensor fluctuations specified at the pivot point $k_{\rm c} = 0.002\,{\rm Mpc}^{-1}$; $R = A_{\rm T}/A_{\rm S}$, the ratio of the amplitude of the scalar fluctuations, $A_{\rm S}$, evaluated at $k_{\rm c} = 0.05\,{\rm Mpc}^{-1}$, and that of the tensor fluctuations evaluated at $k_{\rm c} = 0.002\,{\rm Mpc}^{-1}$. In addition to these parameters, for which we fit, we will also comment on various derived quantities: t_0, the age of the universe; σ_8, the amplitude of density fluctuations in the spheres of $8h^{-1}\,{\rm Mpc}$.

2.2 CMB data

In this paper we will consider the cosmological implications of four different combinations of CMB data.

- The first data set, denoted COBE+VSA contains the VSA data as described in Dickinson et al. (2004) combined with the COBE data (Smoot et al. 1992, Bennett et al. 1996). The purpose of this particular data set is to check the consistency of the VSA data with the concordant model, without imposing the strong constraining power of the WMAP data set (Bennett et al. 2003) .
- The second data set, denoted WMAP contains only the WMAP temperature (TT) data (Hinshaw et al. 2003) and temperature-polarization cross-correlation (TE) data (Kogut et al. 2003). We use these data sets to provide a meaningful comparison with cosmological results obtained from other data sets, avoiding differences that might arise due to the priors and other methodological issues.
- The third data set contains WMAP data and the new VSA data and is referred to as WMAP+VSA. In this dataset we supplement the accurate measurement of the first two peaks by the WMAP satellite with the VSA measurements of the power spectrum in the region between the third and fifth peaks. The importance of these data set is to illustrate the extra information that is available from the measurements of the power spectrum on small angular scales.
- The last data set combines the previous two with all important CMB experiments providing measurements in the region of the second peak of the spectrum and beyond, namely CBI, ACBAR, Boomerang, Maxima, DASI (Pearson et al. 2003; Kuo et al. 2004; Netterfield et al. 2002; Hanany et al. 2002 and Halverson et al. 2002, respectively). This last data set is hereafter referred to as AllCMB.

Throughout our analysis we ignore small correlations between data sets that arise due to the fact that they have observed the same portions of the sky. This applies only to correlations between WMAP, that has used nearly all the sky, and terrestrial experiments, that have observed only small patches. In all cases, the decoupling of observed angular scales and the fact that any given patch of sky observed by a terrestrial experiment makes up less than 1% of the WMAP sky coverage makes this approximation truly valid and far below systematic uncertainties.

2.3 External priors

In addition to the CMB data sets described above, we consider the effects of other cosmological data, not only to break the degeneracies, but also to see how the measured CMB power spectrum fits in the wider cosmological context. Each of these 'external priors' is discussed below.

- The constraint on Hubble's constant obtained by imposing the Hubble Space Telescope (HST) Key project value of $H_0 = 72 \pm 8\,{\rm km\,sec}^{-1}\,{\rm Mpc}^{-1}$ (Freedman et al. 2001) as a Gaussian distribution. The error-bar includes both statistical and systematic uncertainty and prohibits the low density, low h universes allowed by the CMB data alone.
- Constraints on large scale structure from the 2dF Galaxy Redshift Survey (Colless et al. 2001; Percival et al 2001; Percival et al 2002), which provides measurements on scales $0.02 < k/(h\,{\rm Mpc}^{-1}) < 0.15$. The 2dF data measure the power spectrum of the matter fluctuations in the linear regime, which is linked to the spectrum of primordial fluctuations and the parameters of the standard model in a different manner to the CMB data and, thus, provide an important consistency check.
- Constraints from Type Ia Supernovae (SNeIa) (Perlmutter et al. 1999, Reiss et al. 1998), which help to break the CMB geometrical degeneracy and thus accurately determine the ratio of matter to dark-energy components in our Universe.
- Constraints from the gas fraction (f_{gas}) in dynamically relaxed clusters of galaxies (Allen et al. 2002) and from the observed local X-ray luminosity function (XLF) of galaxy clusters (Allen et al. 2003a). These data provide very accurate measurements of matter content of our universe, albeit with large systematic uncertainties.
- Constraints from cosmic shear (CS) measurements (Hoekstra et al. 2002), which provide an independent restriction in the Ω_m-σ_8 plane from that implied by X-ray observations of clusters.

2.4 Parameter estimation

The parameter estimation has been performed using the CosmoMC computer package (Lewis & Bridle 2002) using the April 2003 version of the software (note that the default parametrisation is different in the more recent versions of the CosmoMC package). The calculations were performed

Table 1. Priors used on each cosmological parameter when it is allowed to vary. The notation (a, b) for parameter x denotes a top-hat prior in the range $a \leqslant x \leqslant b$.

Basic Parameter	Prior
$\omega_{\rm b}$	(0.005,0.10)
$\omega_{\rm dm}$	(0.01, 0.99)
h	(0.4,1.0)
$n_{\rm S}, n_1, n_2$	(0.5,1.5)
$z_{\rm re}$	(4,30)
$10^{10} A_{\rm S}$	(10,100)
$n_{\rm run}$	$(-0.15,0.15)$
$A_{\rm X}/(\mu{\rm K})^2$	$(-500,500)$
f_ν	(0,0.2)
$\Omega_{\rm k}$	$(-0.25,0.25)$
w	$(-1.5,0)$
R	(0,2)
$n_{\rm T}$	$(-1.5,3)$

on LAM clusters with a total of 42 CPUs at the IAC in La Laguna, Tenerife and the COSMOS supercomputer facility at the University of Cambridge. The COSMOMC software uses the Markov Chain Monte Carlo (MCMC) algorithm to explore the hypercube of parameters on which we impose flat priors. These priors are listed in Table. 1. Additionally, the software automatically imposes the physical prior $\Omega_\Lambda > 0$, which can significantly affect the marginalized probability distributions (see Slosar et al. 2003 for further discussion). For each considered model, we have run the software until 1 in 25 of samples are accepted. Once this is achieved we ignore the first 200 accepted samples as a burn-in phase. In the flat models this leads to 65000 independent samples, and 200000 in the non-flat case. These samples were then thinned by a factor 25 and used to plot marginalized probability distributions with the GETDIST facility, which is part of the standard COSMOMC package. This program uses a smoothing kernel to infer a sufficiently smooth posterior probability curve from discrete MCMC samples.

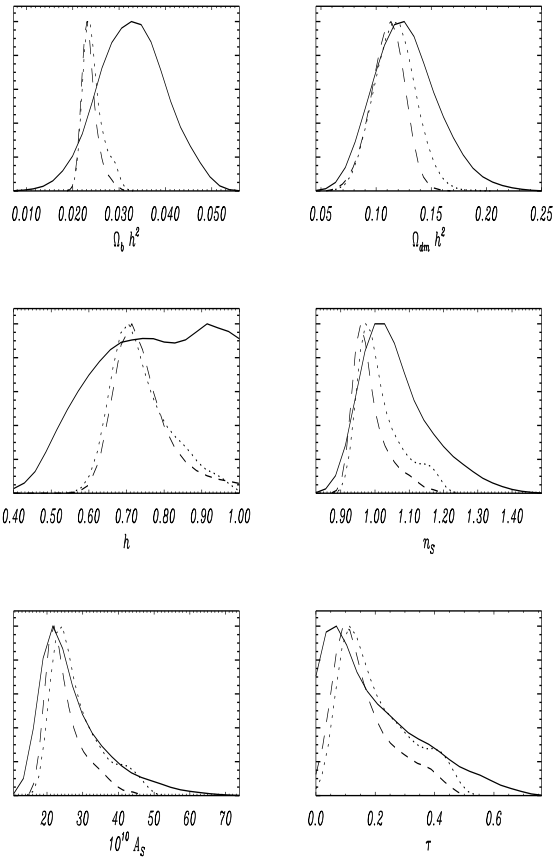

Figure 1. Marginalized distributions for the standard 6-parameter flat ΛCDM model with no external priors (that is, CMB alone) using COBE+VSA (solid-line), WMAP alone (dotted line) and WMAP+VSA (dashed line).

3 RESULTS

3.1 Flat ΛCDM models

3.1.1 Standard six-parameter model

We begin our discussion in the context of the standard flat ΛCDM model with six free parameters ($\omega_{\rm b}$, $\omega_{\rm dm}$, h, $n_{\rm S}$, $A_{\rm S}$, τ), which was discussed in Spergel et al. (2003) for WMAP, with no external priors. We should note that it is, in fact, $z_{\rm re}$ which we allow to vary in our analysis, but we present τ to be consistent with previous work.

The marginalized distributions for the parameters are presented in Fig. 1 and the derived parameter estimates are tabulated in Table 2. The values for WMAP alone can be compared with those in Spergel et al. (2003). Noting that they present $\omega_{\rm m} = \Omega_{\rm m} h^2$, instead of $\omega_{\rm dm}$, there are only minor discrepancies in the central values, although some of the limits appear to be somewhat larger. The preferred value of the redshift of reionization is $z_{\rm re} = 17^{+8}_{-6}$. The inclusion of the high-resolution data from the VSA modifies the limits on each of the parameters as one can see from Fig. 1 and these are most significant for $n_{\rm S}$, whose best fitting value reduces from 1.00 to 0.97. The result for $n_{\rm S}$ will be central to our subsequent discussion of the primordial power spectrum. The results from WMAP+VSA are very similar to those presented in Spergel et al. (2003) for WMAP+ACBAR+CBI.

We have also included in Fig. 1 the marginalized distributions and derived limits obtained from the COBE+VSA data set, all of which show compatibility with the results of WMAP. One slightly unusual result is that for $\omega_{\rm b}$ which is much larger than the value suggested by WMAP, WMAP+VSA and standard Big Bang Nucleosynthesis, $\omega_{\rm b} = 0.020 \pm 0.002$, (Burles, Nollett and Turner 2001) and is a result of somewhat larger amplitude of the 3rd peak and the shifted first peak preferred by the VSA data (Rubiño-Martin et al. 2003) in isolation (see Dickinson et al. 2004 for a detailed discussion of the preferred peak structure of the current data). Comparing the derived distributions with those obtained by Slosar et al. 2003 (using the earlier VSA data presented in Grainge et al. 2003), we find that the results are fully consistent, but the additional VSA data has led to tighter parameter constraints. In particular, the upper limit on $\omega_{\rm dm}$ has been significantly reduced.

Table 2. Parameter estimates and 68% confidence limits for the standard six-parameter flat ΛCDM model.

Parameter	COBE+VSA	WMAP	WMAP+VSA
$\omega_{\rm b}$	$0.0328^{+0.0073}_{-0.0071}$	$0.0240^{+0.0027}_{-0.0016}$	$0.0234^{+0.0019}_{-0.0014}$
$\omega_{\rm dm}$	$0.125^{+0.031}_{-0.027}$	$0.117^{+0.018}_{-0.018}$	$0.111^{+0.014}_{-0.016}$
h	$0.77^{+0.15}_{-0.17}$	$0.73^{+0.10}_{-0.06}$	$0.73^{+0.09}_{-0.05}$
$n_{\rm S}$	$1.05^{+0.12}_{-0.08}$	$1.00^{+0.09}_{-0.04}$	$0.97^{+0.06}_{-0.03}$
$10^{10}A_{\rm S}$	25^{+11}_{-6}	27^{+9}_{-5}	23^{+7}_{-3}
τ	Unconstrained	$0.18^{+0.16}_{-0.08}$	$0.14^{+0.14}_{-0.07}$

Table 3. Limits on $n_{\rm S}$ and $n_{\rm run}$ in the flat ΛCDM model with a running spectral index for different CMB data sets and external priors.

CMB	External	$n_{\rm S}$	$n_{\rm run}$
COBE+VSA	None	$0.93^{+0.13}_{-0.12}$	$-0.081^{+0.049}_{-0.049}$
WMAP	None	$0.94^{+0.07}_{-0.06}$	$-0.060^{+0.037}_{-0.036}$
WMAP+VSA	None	$0.96^{+0.07}_{-0.07}$	$-0.069^{+0.032}_{-0.032}$
COBE+VSA	HST	$0.92^{+0.11}_{-0.12}$	$-0.081^{+0.048}_{-0.048}$
WMAP	HST	$0.95^{+0.06}_{-0.07}$	$-0.060^{+0.037}_{-0.037}$
WMAP+VSA	HST	$0.93^{+0.06}_{-0.05}$	$-0.069^{+0.036}_{-0.036}$
COBE+VSA	2dF	$1.00^{+0.12}_{-0.13}$	$-0.044^{+0.058}_{-0.061}$
WMAP	2dF	$0.95^{+0.05}_{-0.06}$	$-0.038^{+0.025}_{-0.037}$
WMAP+VSA	2dF	$0.93^{+0.05}_{-0.05}$	$-0.049^{+0.035}_{-0.034}$

3.1.2 Running spectral index models

In the previous section we saw that the inclusion of the VSA data to that of WMAP shifts the derived limits on the spectral index. Standard, slow-roll models of inflation predict that the spectral index will be a function of scale, albeit at a very low level, and it seems a sensible parameter to allow as the first beyond the standard model. The analysis of Spergel et al. (2003) and Peiris et al. (2003) provided evidence for a non-zero value of $n_{\rm run}(=-0.031^{+0.016}_{-0.017})$ when using CMB data from WMAP, ACBAR and CBI, along with large-scale structure data from the 2dF galaxy redshift survey and the Lyman-α forest. This result was discussed independently by Bridle et al. (2003), Barger et al. (2003), Leach & Liddle (2003), Kinney et al. (2003), where it is was shown that it was highly dependent on the inclusion of the data from the Lyman-α forest, the veracity of which has been questioned (Seljak et al. 2003).

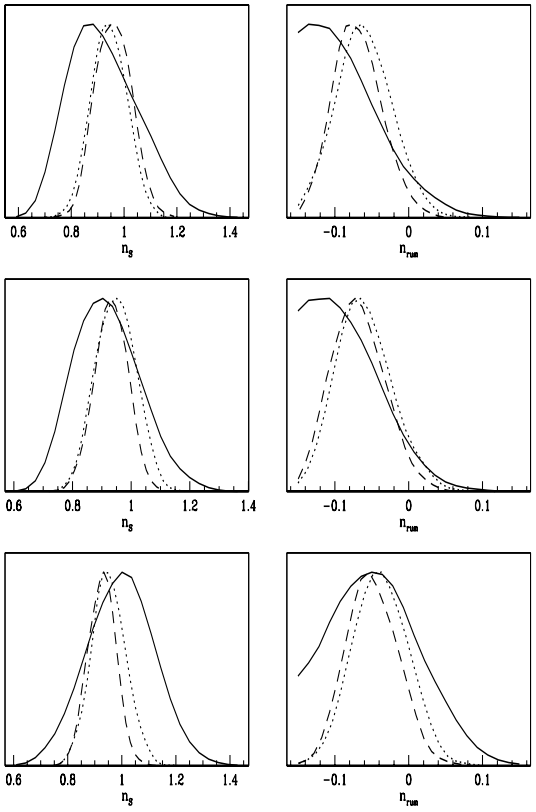

Figure 2. Marginalized distributions for $n_{\rm S}$ and $n_{\rm run}$ in the flat ΛCDM model with a running spectral index. Line-styles are as in Fig. 1. The external priors adopted are: none (top row), HST (middle row), 2dF (bottom row).

We will start our discussion by considering the same model as in the previous section with no external priors, but with $n_{\rm run}$ allowed to vary. The marginalized distributions and derived limits on $n_{\rm S}$ and $n_{\rm run}$ are presented in the top row of Fig. 2 and the first three rows of Table 3 for COBE+VSA, WMAP and WMAP+VSA. The derived limits on $\omega_{\rm b}$, $\omega_{\rm dm}$ and h are not changed appreciably and the other parameters, $A_{\rm S}$ and τ (or $z_{\rm re}$) are strongly degenerate and $z_{\rm re}$ will feature in our discussion below.

The values of $n_{\rm S}$ and $n_{\rm run}$ are not particularly well constrained by COBE+VSA, but it is worth noting that even in this case there is a definite preference for a value of $n_{\rm run} < 0$. The results have been included for completeness and provide a useful cross-check. The results for WMAP are somewhat different to those presented in Spergel et al. (2003), something to which we will return in the subsequent discussion. In particular we find that $n_{\rm run} = -0.060^{+0.037}_{-0.036}$, a 1.6σ preference for $n_{\rm run} < 0$, as opposed to $n_{\rm run} = -0.047 \pm 0.04$ from Spergel et al. (2003). The significance of this result is improved to 2.2σ by the inclusion of the high resolution data from the VSA. These quantitative results are borne out on

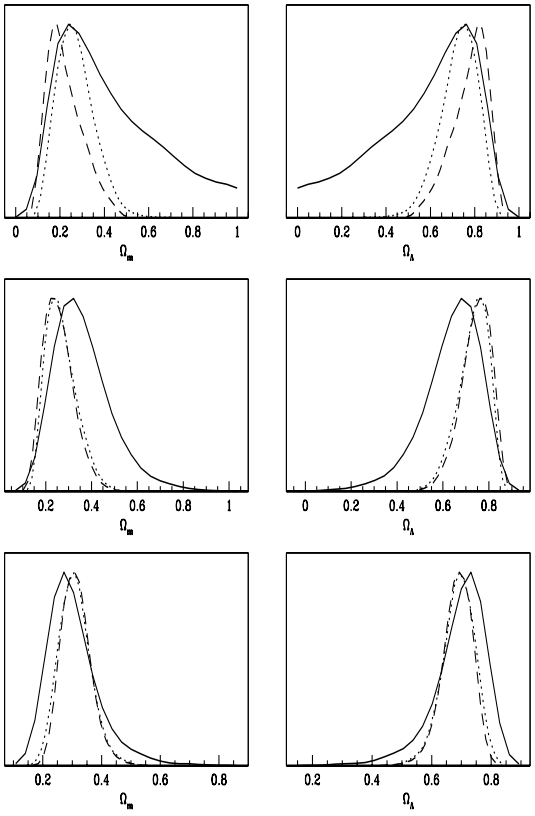

Figure 3. As for Fig. 2, but for the parameters $\Omega_{\rm m}$ and Ω_Λ.

examination of the likelihood curves. It is worth emphasizing that this result comes from CMB data alone.

We have tested the sensitivity of this apparently strong result to the inclusion of external priors from the HST and 2dF galaxy redshift survey, and the results are also presented in Fig. 2 and Table 3. We see that the effect of the HST prior is to relax marginally the constraint on $n_{\rm run}$, although there is a significant change in the derived limit on $n_{\rm S}$. We note that the results for WMAP alone are very similar with and without the HST prior.

The inclusion of 2dF does significantly affect our results. Using just WMAP we find that there is only a marginal preference for $n_{\rm run} < 0$ and the inclusion of VSA only yields a 1.4σ result. We note that this is a shift in the derived value and the error bars do not change significantly; it is worth discussing the reason for this shift since it is due to the breaking of a degeneracy by the addition 2dF data. The main parameter combination which is constrained by the galaxy power spectrum is the shape parameter $\Gamma = \Omega_{\rm m} h$ which arises from the size of the horizon at matter-radiation equality measured in redshift space. Hence, once combined with the CMB data the derived parameters $\Omega_{\rm m}$ and Ω_Λ are constrained individually (Efstathiou et al. 2002). Fig. 3 presents the marginalized distribution for these parameters for the three cases: no external prior, HST prior and 2dF prior. We see that for the first two cases, in which there is significant evidence for $n_{\rm run} < 0$, the preferred values of $\Omega_{\rm m}$

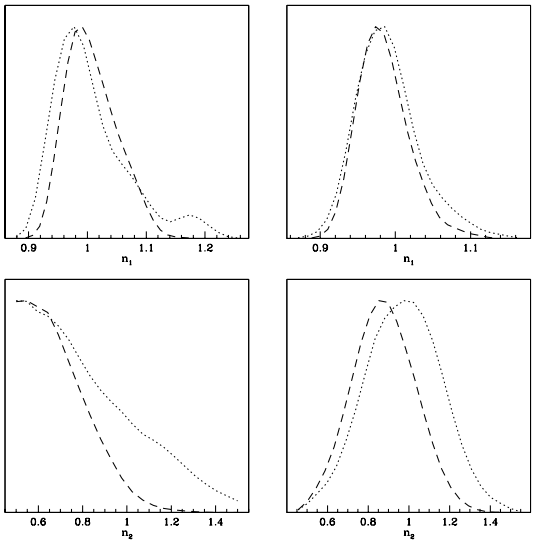

Figure 4. Marginalized distributions for n_1 and n_2 in the flat ΛCDM model with a broken power-law index. The line styles are as in Fig. 1. The left-hand column assumes the HST prior and the right-hand column assumed the 2dF prior.

are much lower (extremely low in the no prior case) with the corresponding mean values of the distributions giving $\Omega_{\rm m} h \approx 0.17 - 0.18$, whereas in the latter case $\Omega_{\rm m} \approx 0.3$, $h \approx 0.68$ and $\Omega_{\rm m} h \approx 0.21$, closer to the value suggested by Percival et al. (2001) from the their analysis of the 2dF alone.

We have also considered the effects of including other CMB information from the two other high resolution experiments ACBAR and CBI. We find that the inclusion of their results does not appear to be as significant as the VSA in preferring a value of $n_{\rm run} < 0$ and that the result of considering WMAP+ACBAR+CBI+VSA is very similar to just WMAP+VSA. We note that the ACBAR and CBI experiments quote large global calibration uncertainties (20% and 10% in power), which we believe is at least as responsible for this result as their errors on the individual power spectrum band powers. We note that the calibration uncertainty for the CBI is likely to improve for future data in a similar way as for the VSA. A future re-calibration of CBI and more data are likely to address this issue (C. Contaldi, priv. comm.).

3.1.3 Broken power law models

In the previous section we have seen that there is some evidence for an initial power spectrum of density fluctuations which is not described by a single power law index. The running spectral index model is suggested by slow-roll inflation. However, the values which are preferred by the data, at least with some priors, are too large to come from standard slow-roll inflation and are incompatible with the idea of the spectral index being a power series in $\log(k/k_{\rm c})$. Here, we consider a model with two spectral indices n_1 and n_2, with the cross-over point being $k_{\rm c} = 0.05\,{\rm Mpc}^{-1}$.

The results obtained from this model are presented in

Fig. 4 for the HST and 2dF external priors respectively, using CMB data from WMAP and WMAP+VSA. We see that, in both cases and with both datasets, one obtains $n_1 \approx 1$. The situation for n_2 is more complicated. For the HST case (left column) we see that the best fitting value is very low. In fact, it is lower than the lower limit we have included as a top hat prior. For WMAP values as large as $n_2 = 1.4$ are not excluded, whereas the inclusion of the VSA has the effect of excluding models with $n_2 > 1$. The inclusion of the 2dF prior (right column) has a strong effect, moving the distribution of n_2 to larger values, but still preferring $n_2 < 1$. In this case for WMAP we find that $n_1 = 0.99 \pm 0.04$ and $n_2 = 0.97 \pm 0.18$ which suggests that something close to scale-invariant $n_1 = n_2 = 1$ is preferred, whereas for WMAP+VSA $n_1 = 0.99 \pm 0.03$ and $n_2 = 0.88 \pm 0.15$. While this is clearly compatible with scale invariant even at the 1σ level, there is undoubtedly a preference for a broken spectral index when the VSA is included.

It is clear that our results are compatible with those of the previous section on running spectral index models. Models with $n_{\rm run} < 0$ have a lower value of the spectral index for $k > k_{\rm c}$ than for $k < k_{\rm c}$ and this is exactly what we find in this alternative parameterization. We should note that large variations in n_2 only lead to much smaller changes in the actual power spectrum than one might expect naively from, for example, plotting the power spectrum for different values of $n_{\rm S}$ within the standard ΛCDM model.

3.1.4 Neutrino fraction

As a final extension to our flat ΛCDM model, it is of interest to include the fraction f_ν of dark matter in the form of neutrinos. Evidence for a neutrino oscillation, and hence for the existence of massive neutrinos, has been found by solar neutrino and atmospheric neutrino experiments (Fukuda et al. 1998, 2002; Allison et al. 1999; Ambrosio et al. 2000; Ahmad et al. 2002). Further evidence for a non-zero value of the neutrino mass has recently been claimed from cosmological data (Allen et al. 2003b).

In addition to obtaining constraints on f_ν, the inclusion of this parameter will inevitably lead to some broadening of the marginalized distributions for the other parameters. Of particular interest is whether the constraints on the running spectral index derived above are robust to the inclusion of f_ν. We therefore include f_ν, with the top-hat prior given in Table 1, into the running spectral index model. In the analysis of this model, we include the 2dF external prior, since current CMB alone provide only a weak constraint on f_ν.

Fig. 5 shows the marginalized distributions obtained for f_ν, $n_{\rm S}$ and $n_{\rm run}$ for the three CMB data sets COBE+VSA, WMAP and WMAP+VSA. We find that the 95% upper limit provided by the COBE+VSA data set, $f_\nu < 0.132$, is only marginally larger than that obtained using WMAP data, $f_\nu < 0.090$. The combination WMAP+VSA gives similar limits to WMAP, namely $f_\nu < 0.087$, which corresponds to neutrino mass of $m_\nu < 0.32$eV when the neutrino masses are degenerate.

For the parameters $n_{\rm S}$ and $n_{\rm run}$, we see that, as compared with those plotted in Fig. 2 (middle row), the marginalized distributions have indeed been shifted and broadened by the inclusion of f_ν although the effects are not very strong. In particular, we note that our earlier finding of a preference for a non-zero value of $n_{\rm run}$ has been weakened somewhat. A non-zero $n_{\rm run}$ is still preferred, but at reduced significance. For the WMAP+VSA data set, we obtain $n_{\rm S} = 0.94^{+0.06}_{-0.06}$ and $n_{\rm run} = -0.041^{+0.037}_{-0.036}$ with 68% confidence limits.

In the above analysis we used only 2dF as an external prior. It is of interest to investigate the effect of including different combinations of the additional external priors listed in Table 1. The effect of these additional priors has been calculated by importance sampling our previous results. We also investigate the effect of including all recent CMB data into our analysis. In Fig. 6, we plot confidence limits on all the model parameters for each of our four CMB data sets, each of which, in turn, includes four different combinations of external priors: 2dF, 2dF+$f_{\rm gas}$, 2dF+$f_{\rm gas}$+XLF, 2df+HST and 2dF+CS. The points indicate the median of the corresponding marginalized distribution, and the error bars show the 68% central confidence limit. If the distribution peaks at zero, the point is placed on the axis and the 95% upper limit is shown.

We see that the inclusion of the $f_{\rm gas}$ and XLF external priors significantly reduces the error bars on all parameters. The most profound effect is obtained from the XLF prior for the parameters f_ν, σ_8 and $z_{\rm re}$, as might be expected from Allen et al. (2003b). Indeed, it is only with the inclusion of the XLF prior that a non-zero value of f_ν is preferred and only then at limited significance. For each of the CMB data set combinations, the best-fitting value in this case is $f_\nu \approx 0.05$, which corresponds to neutrino mass of $m_\nu \approx 0.18$eV when the neutrino masses are degenerate, with a zero value excluded at around 96% confidence. For σ_8 the inclusion of the XLF prior significantly reduces the best-fit value and the error bars for all CMB data set combinations. A similar, but less pronounced, effect is seen for $z_{\rm re}$.

3.2 General ΛCDM model

Thus far we have considered only a limited range of flat ΛCDM models. In principle, one should properly include all the relevant unknowns into the analysis in order to obtain conservative confidence limits. In this section, we consider a more general ΛCDM model. In addition to including f_ν and $n_{\rm run}$, the standard six-parameter flat ΛCDM model is further extended by including Ω_k, w, $R = A_{\rm T}/A_{\rm S}$ and $n_{\rm T}$. This gives 12 variable parameters in total, for which we adopt the top-hat priors listed in Table 1.

For this model, we consider the three CMB data sets WMAP, WMAP+VSA and AllCMB. In addition, we now use both 2dF and SNeIa as our basic external priors, which are required in order to set constraints on our 12-dimensional cosmological parameter space. For each CMB data set, the marginalized distributions for each parameter are shown in Fig. 7. In addition, marginalized distributions are plotted for the derived parameters Ω_Λ, $\Omega_{\rm m}$, t_0 and σ_8. The corresponding confidence limits on the parameter values are given in Table 4.

In this more general model we see that the marginalized distributions of the parameters in our simpler models have broadened somewhat, but are still consistent with our earlier findings. Perhaps most interesting is the fact that some of the marginalized distributions change considerably as more

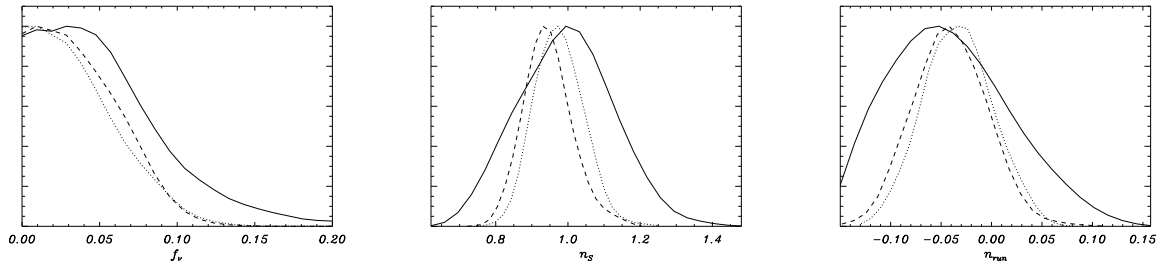

Figure 5. Marginalized distributions for f_ν, n_s and $n_{\rm run}$ in the extended flat ΛCDM model, using the 2dF external prior and COBE+VSA (solid-line), WMAP alone (dotted line) and WMAP+VSA (dashed line).

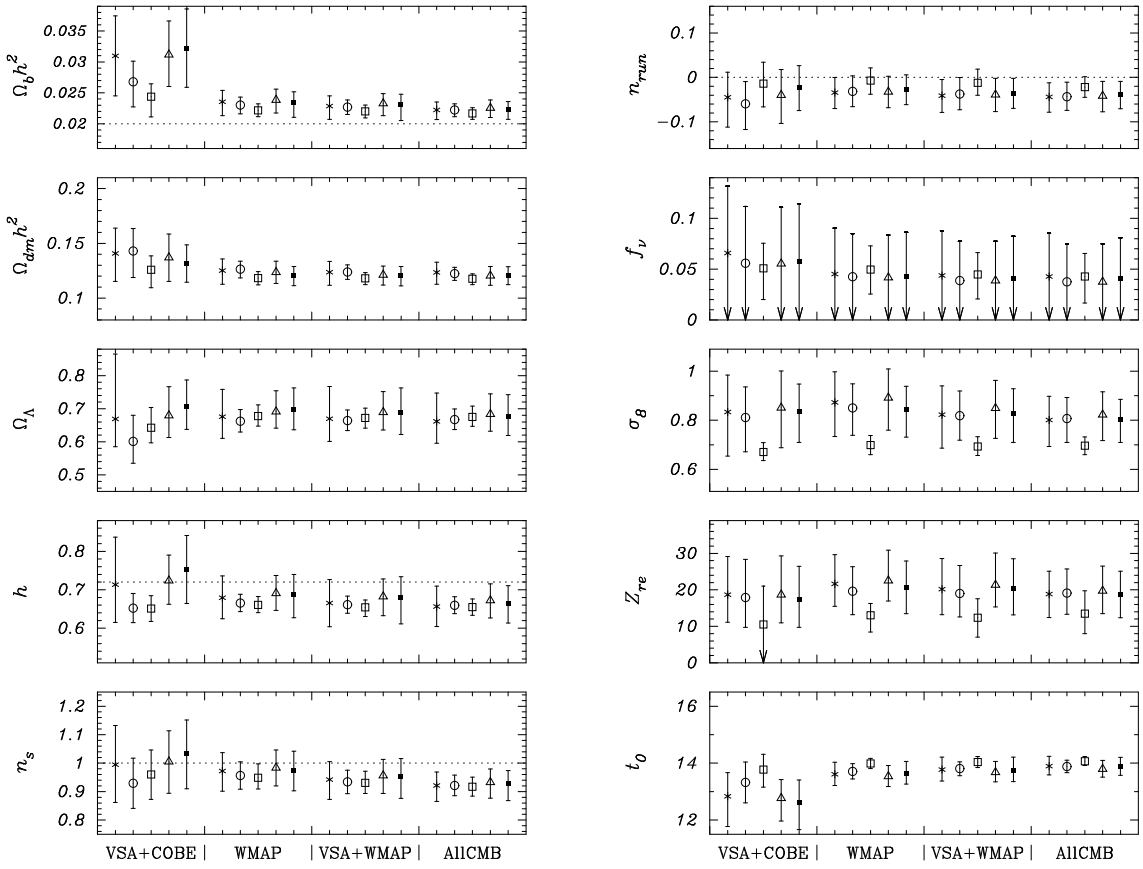

Figure 6. Estimates for cosmological parameters in the flat ΛCDM running spectral index model, extended to include f_ν. Four CMB data sets are considered and, for each data set, four determinations are plotted, corresponding to different combinations of external priors. From left to right the external priors are: 2dF; 2dF+$f_{\rm gas}$; 2dF+$f_{\rm gas}$+XLF; 2dF+HST and 2dF+CS. The points indicate the median of the corresponding marginal distributions. The error bars denote 68% confidence limits. If a distribution peaks at zero then the 95% upper limit is shown. The horizontal dashed lines plotted in some of the panels indicate BBN values for $\Omega_{\rm b}h^2$, the value of h given by the HST key project, the Harrison-Zel'dovich value of the spectral index of fluctuations and a zero value for the running index.

CMB data are used beyond WMAP. For $\Omega_{\rm b}h^2$ we see a clear trend towards a lower preferred value (closer to the BBN estimate) as one adds first VSA data and then all remaining CMB data sets. This effect is accompanied by a gradual upwards trend in the preferred $\Omega_{\rm dm}h^2$ value. The other parameters exhibiting such trends are $n_{\rm S}$ and $n_{\rm run}$. As more CMB data are included, the preferred value of $n_{\rm S}$ moves slightly below unity, although this value is by no means excluded. Perhaps more importantly, the upper limit on $n_{\rm S}$ is significantly reduced as more CMB data are added. An analogous effect is observed for $n_{\rm run}$, for which the addition of VSA data significantly reduces the tail of the distribution for positive values of $n_{\rm run}$.

The remaining marginalized distributions have very similar forms for each of the three CMB data sets, indicating that, for these parameters, the addition of further CMB beyond WMAP does not have a significant effect on their derived values and confidence limits. It is worth noting in passing, however, that all CMB data sets are fully consistent with a zero curvature model. Moreover, we find

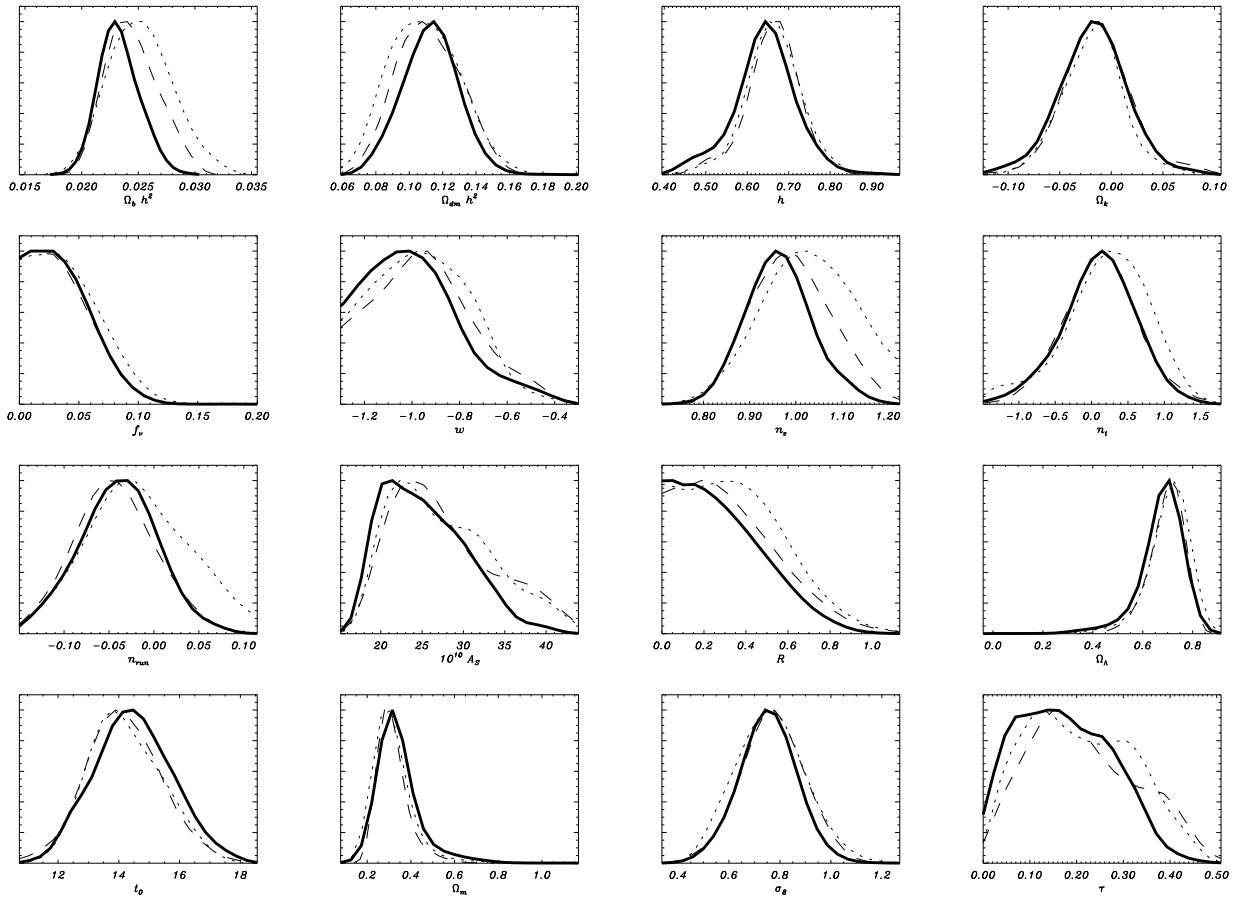

Figure 7. Marginalized distributions for various cosmological parameters in the 12-parameter general non-flat ΛCDM model from WMAP (dotted line), WMAP+VSA (dashed line) and AllCMB (thick solid line) in combination with external priors from both 2dF and SNeIa.

$w = -1$ with an uncertainty of ± 24%, which is consistent with dark energy in the form of a cosmological constant. As regards inflation models, we find that the inclusion of VSA data makes a modest reduction in the upper limit on the tensor-to-scalar ratio, which is reduced still further (albeit marginally) by the inclusion of all CMB data; in this last case we obtain $R < 0.68$ at 95% confidence. The power-law index of tensor modes $n_{\rm T}$ is fully consistent with zero.

As we did for the flat ΛCDM model, we may investigate the effect of including additional external priors in our analysis of the general model. In Fig. 8 we plot the confidence intervals on all the model parameters for each of our four CMB data sets, each of which, in turn, includes four different combinations of external priors: 2dF, 2dF+$f_{\rm gas}$, 2dF+$f_{\rm gas}$+XLF, 2dF+HST and 2dF+CS. Once again, we see that the inclusion of the $f_{\rm gas}$ and XLF external priors has the greatest effect on the confidence limits, and that this is most pronounced for the XLF prior and the parameters f_ν, σ_8 and $z_{\rm re}$. It is reassuring, however, that the derived limits on f_ν for the general model are very similar to those obtained assuming the simpler flat model. We again find $f_\nu \approx 0.05$, with a zero-value excluded at about 92% confidence which is slightly lower than for the flat case. The effect of the XLF prior on σ_8 and $z_{\rm re}$ in the general model is also similar to that observed in the simpler flat case.

4 DISCUSSION AND CONCLUSIONS

We have used recent data from the Very Small Array, together with other CMB datasets and external priors, to set constraints on cosmological parameters. We have considered both flat and non-flat ΛCDM models and the results are consistent.

Within the flat ΛCDM model, we find that the inclusion of VSA data suggests that the initial fluctuation spectrum that is not described by a single power-law. As we have pointed out already, the value of $n_{\rm run}$ preferred by the data is incompatible with the basic premises of slow-roll inflation. Moreover, the negative running, which reduces the amount of power on small scales and hence the amount of structure at early times, leads to predictions for the epoch of reionization at odds with the best fit to the CMB data. This comes almost directly from the temperature-polarization cross-correlation power spectrum observed by WMAP (Kogut et al. 2003). Given the implications of this result it is important to consider the possible systematic effects that might weaken it.

The absolute calibration uncertainty of the VSA power spectrum is an important contributory factor to this result. The 3% uncertainty quoted in Dickinson et al. (2004) relies heavily on the the measurement of the temperature of Jupiter, $T_{\rm jup}$, by WMAP and this requires an overall factor

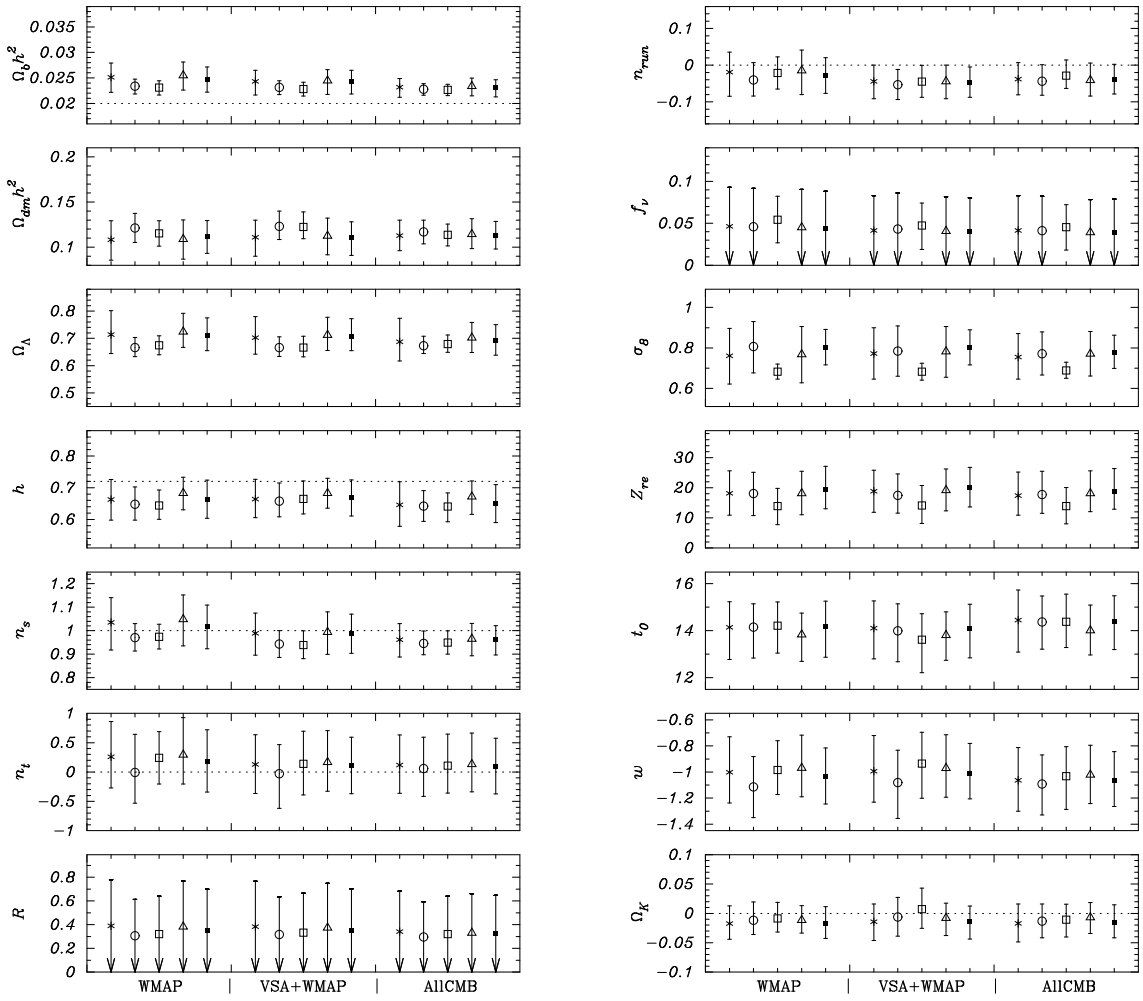

Figure 8. As for Fig. 6, but for the general 12-parameter non-flat ΛCDM model.

of 0.92 modification in the power spectrum estimates from the previous VSA results (Grainge et al 2003; Scott et al 2002) which were reliant on on earlier measurements of $T_{\rm jup}$ given by Mason et al. (1999). It was pointed out in Dickinson et al. that, in fact, using an absolute calibration based on this measurement of $T_{\rm jup}$ gives the most consistent normalization of the power spectrum when compared to that of WMAP.

We have investigated the effects of possible uncertainties in the calibration in two ways. First, we consider the possibility of using the Mason et al (1999) central value for $T_{\rm jup}$ while maintaining an overall uncertainty of 3%. As an alternative we just increase the overall uncertainty in the calibration to 10% while keeping the central value for $T_{\rm jup}$ from WMAP. The derived limits on $n_{\rm S}$ and $n_{\rm run}$ are presented in Table 5 for these two possibilities using the HST and 2dF priors. We see in each case that the preference for $n_{\rm run} < 0$ is weakened to below 2σ compared to the calibration based on WMAP's measurement of $T_{\rm jup}$. It is clear that refinement of the absolute calibration of the VSA in the light of the WMAP measurements is something requiring further attention.

Another possible systematic effect is the residual point source correction due to sources below out subtraction limit of 20mJy. This was computed by normalizing the point source model of Toffolatti et al. (1998) to the observed VSA source counts which can then be extrapolated to lower flux densities. There are clearly some uncertainties in this procedure. It is possible that an imperfect subtraction, either an over-estimate or an under-estimate, could lead to inaccuracies in the derived limits on the cosmological parameters, in particular on $n_{\rm S}$ and $n_{\rm run}$. In order to investigate possible effects of such uncertainties we have performed our likelihood analysis with the inclusion of the parameter $A_{\rm X}$ which was discussed in section 2.1. We note that it is also possible that for Galactic foregrounds might contribute to this. However, it was shown in Dickinson et al. (2004) that the level of foreground contamination of the VSA fields was negligible.

We find that the derived limits on $n_{\rm S}$ and $n_{\rm run}$ in this case are less stringent than without including $A_{\rm X}$ for WMAP+VSA. The marginalized distributions for $n_{\rm S}$, $n_{\rm run}$ and $A_{\rm X}$ are presented using CMB data from WMAP and WMAP+VSA for the external priors from HST and 2dF in Fig. 9 and the derived limits are presented in Table. 6. In fact the likelihood curves and derived limits for WMAP and WMAP+VSA are almost identical when $A_{\rm X}$ is included in the analysis and the WMAP limits are very similar to when $A_{\rm X}$ is constrained to be zero (see Table 3). We see that there

Table 5. Limits on $n_{\rm S}$ and $n_{\rm run}$ in the flat ΛCDM model with a running spectral index for different absolute calibration schemes. The uncertainty refers to that in the power. See text for discussion.

$T_{\rm jup}$	Uncertainty	External	$n_{\rm S}$	$n_{\rm run}$
Mason et al.	3%	HST	$0.93^{+0.05}_{-0.05}$	$-0.058^{+0.038}_{-0.038}$
Mason et al.	3%	2dF	$0.93^{+0.05}_{-0.05}$	$-0.028^{+0.047}_{-0.047}$
WMAP	10%	HST	$0.93^{+0.05}_{-0.05}$	$-0.055^{+0.035}_{-0.035}$
WMAP	10%	2dF	$0.95^{+0.06}_{-0.06}$	$-0.040^{+0.033}_{-0.033}$

Table 4. Parameter estimates and 68% confidence intervals for various cosmological parameters as derived from Fig. 7. For f_ν and R, the 95% upper limits are quoted.

	WMAP	WMAP+VSA	AllCMB
$\Omega_{\rm b}h^2$	$0.025^{+0.003}_{-0.003}$	$0.024^{+0.003}_{-0.002}$	$0.023^{+0.002}_{-0.002}$
$\Omega_{\rm dm}h^2$	$0.108^{+0.022}_{-0.021}$	$0.111^{+0.021}_{-0.019}$	$0.113^{+0.017}_{-0.017}$
h	$0.66^{+0.07}_{-0.06}$	$0.66^{+0.06}_{-0.06}$	$0.65^{+0.07}_{-0.07}$
$z_{\rm re}$	18^{+7}_{-7}	19^{+7}_{-7}	17^{+7}_{-8}
$\Omega_{\rm k}$	$-0.02^{+0.03}_{-0.03}$	$-0.01^{+0.03}_{-0.03}$	$-0.02^{+0.03}_{-0.03}$
f_ν	< 0.093	< 0.083	< 0.083
w	$-1.00^{+0.24}_{-0.27}$	$-0.99^{+0.24}_{-0.27}$	$-1.06^{+0.24}_{-0.25}$
$n_{\rm S}$	$1.04^{+0.12}_{-0.11}$	$0.99^{+0.09}_{-0.09}$	$0.96^{+0.07}_{-0.07}$
$n_{\rm T}$	$0.26^{+0.53}_{-0.60}$	$0.13^{+0.49}_{-0.51}$	$0.12^{+0.48}_{-0.51}$
$n_{\rm run}$	$-0.02^{+0.07}_{-0.05}$	$-0.04^{+0.05}_{-0.04}$	$-0.04^{+0.04}_{-0.05}$
$10^{10}A_{\rm S}$	27^{+8}_{-5}	26^{+9}_{-5}	25^{+6}_{-5}
R	< 0.78	< 0.77	< 0.68
Ω_Λ	$0.71^{+0.07}_{-0.09}$	$0.70^{+0.06}_{-0.08}$	$0.69^{+0.07}_{-0.09}$
t_0	$14.1^{+1.4}_{-1.1}$	$14.1^{+1.3}_{-1.2}$	$14.4^{+1.4}_{-1.3}$
$\Omega_{\rm m}$	$0.31^{+0.09}_{-0.07}$	$0.31^{+0.08}_{-0.06}$	$0.33^{+0.10}_{-0.07}$
σ_8	$0.76^{+0.14}_{-0.14}$	$0.77^{+0.13}_{-0.13}$	$0.76^{+0.11}_{-0.12}$
τ	$0.20^{+0.13}_{-0.11}$	$0.20^{+0.15}_{-0.10}$	$0.17^{+0.12}_{-0.10}$

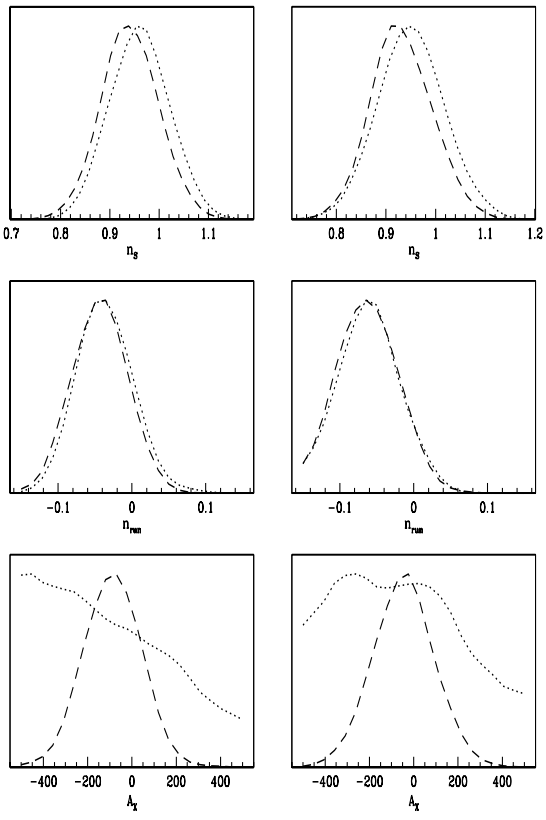

Figure 9. Marginalized distributions for $n_{\rm S}$, $n_{\rm run}$ and $A_{\rm X}$ when $A_{\rm X}$ is allowed to vary. The line-styles are as in Fig. 1. but COBE+VSA is excluded The left-hand column is for the HST prior and the right-hand for the 2dF prior.

are essentially no limits on $A_{\rm X}$ when just considering WMAP and that in the case of WMAP+VSA, $A_{\rm X}$ is compatible with zero suggesting that to within at least $\approx 100(\mu{\rm K})^2$ the source subtraction procedure has been successful. For the HST prior $A_{\rm X} < 214\,(\mu{\rm K})^2$ at 95% confidence and for the 2dF prior $A_{\rm X} < 155\,(\mu{\rm K})^2$.

Assuming that the subtraction is perfect and that the

Table 6. Limits on $n_{\rm S}$, $n_{\rm run}$ and $A_{\rm X}$ in the flat ΛCDM model with a running spectral index when the parameter $A_{\rm X}$ is included. The final column is the 95% confidence upper limit on $A_{\rm X}$. The units of $A_{\rm X}$ are in $(\mu K)^2$.

CMB	External	$n_{\rm S}$	$n_{\rm run}$	$A_{\rm X}$	$A_{\rm X}\,(2\sigma)$
WMAP	HST	$0.95^{+0.06}_{-0.06}$	$-0.059^{+0.039}_{-0.039}$	Unconstrained	
WMAP+VSA	HST	$0.93^{+0.06}_{-0.06}$	$-0.061^{+0.038}_{-0.038}$	-46 ± 132	< 214
WMAP	2dF	$0.96^{+0.06}_{-0.06}$	$-0.036^{+0.036}_{-0.036}$	Unconstrained	
WMAP+VSA	2dF	$0.94^{+0.06}_{-0.06}$	$-0.043^{+0.035}_{-0.035}$	-86 ± 123	< 155

SZ contribution to the power spectrum is $\propto \ell^2$ for $\ell < 4000$ then our results on $A_{\rm X}$ can be used to derive a limit on $(\Delta T_\ell)^2$ in a bandpower, B_{3000}, covering $2000 \leqslant \ell \leqslant 4000$ as observed by CBI. Under the assumption that $\Delta T_\ell \propto \ell^2$, we find that

$$B_{3000} = \frac{28}{3} A_{\rm X}\,. \qquad (5)$$

This leads to a limit of $B_{3000} < 1997\,(\mu{\rm K})^2$ using the HST prior and $B_{3000} < 1446\,(\mu{\rm K})^2$ for the 2dF prior. The value quoted by Mason et al. (2003) is $B_{3000} = (508 \pm 168)\,(\mu{\rm K})^2$ which is more stringent than our limit. However, this value and our limit are derived in very different ways. The measurement of Mason et al. (2003) is a direct limit from high resolution imaging of 3 deep fields. While it is direct, the measurement the global power spectrum could be significantly affected by sample variance; one could have observed a field which in there are more clusters than the global average and hence obtain a biased estimation of the global power spectrum. Our limit is indirect, coming from the power spectrum measured over 82 deg^2 at lower angular resolution and it requires that the power spectrum be $\propto \ell^2$ as well as the cosmological model to be correct. It is likely that this represents a reliable upper bound since the power spectrum will grow less rapidly than ℓ^2 for $\ell > 1500$ due to the fact that the clusters responsible for the SZ effect are not point sources. Moreover, it is not as sensitive to the Poisson distributed number of clusters in an individual field. A more realistic modelling of the SZ effect using accurate power spectra could yield a more stringent upper bound. The two methods provide useful complimentary information and it is possible that a much more stringent constraint on $A_{\rm X}$ will be possible when the VSA observes with higher resolution in the near future.

One important feature of the power spectrum observed by WMAP is the apparent absence of power at very low ℓ. This could be due to some as yet unknown physics, or it could be a manifestation of the interaction between the subtle systematic effects caused by the side-lobes, the Galactic cut, and the power spectrum estimation algorithm used by the WMAP team (Efstathiou 2003). It is worth assessing to what extent our result is dependent on the measured anisotropies with $\ell < 10$. By excluding the multipoles with $\ell < 10$ from our analysis we find that $n_{\rm S} = 1.01 \pm 0.07$ and $n_{\rm run} = 0.007 \pm 0.049$, strongly suggestive of an $n_S \equiv 1$, scale invariant initial power spectrum for WMAP with the 2dF prior, whereas $n_{\rm S} = 0.97 \pm 0.06$ and $n_{\rm run} = -0.015 \pm 0.047$ for WMAP+VSA and the same prior. The weakening of the constraint on $n_{\rm run}$ should not be a surprise since excluding multipoles with $\ell < 10$ cuts out nearly a whole power of ten in k and $n_{\rm run}$ is the coefficient of a power series in $\log(k/k_{\rm c})$. However, we see that the inclusion of the VSA tends to prefer a spectral index lower than just WMAP. It is clear from this that the reason for the preference for a negative running of the power spectrum when multipoles with $\ell < 10$ are included is the tension between the measurements at $\ell < 10$ by WMAP and for $\ell > 1000$ by the VSA.

We should comment briefly on one aspect of our analysis of the running spectral index models which is not ideal: the preferred values of $z_{\rm re}$ and τ. Most recent analyses of CMB data include an upper bound one of these parameters. In Spergel et al. (2003) a flat prior of $\tau < 0.3$ was used when in some cases the data had a preference for a high value of τ by virtue of the low-ℓ TE correlation power spectrum; our analysis is no different and we believe that this is responsible for the differences between our analysis and that of Spergel et al (2003). All the likelihood curves and derived limits have made the not unreasonable assumption that $z_{\rm re} < 30$. However, in some cases, particularly those for which we have included no prior from 2dF, the preferred values of $z_{\rm re}$ are close to this limit, uncomfortably close in some cases and one might be concerned that our results are sensitive to this. We find that the models with $n_{\rm run}$ significantly less than zero tend to have larger values of $z_{\rm re}$ which explains why our derived limit of $n_{\rm run} = -0.060 \pm 0.037$ from WMAP is larger than the one quoted in Spergel et al (2003). It also suggests that, by excluding $z_{\rm re} > 30$, we have weakened the constraint on $n_{\rm run}$ rather than artificially modifying the preferred value away from zero. An epoch of reionization with $z_{\rm re} \approx 30$ would seem unlikely in the context of early structures being the source of ionization, but it is clear that the data suggest it.

For the general 12-parameter ΛCDM model, we find that our marginalized distributions for $n_{\rm S}$ and $n_{\rm run}$ are broadened, as one would expect. Nevertheless, even in this case, the addition of VSA data significantly reduces tails of the distributions for $n_{\rm S}$ greater than unity and for positive $n_{\rm run}$, as compared with using WMAP as the only CMB

data set. Indeed, these effects are reinforced by the use of the AllCMB data set. The inclusion of additional CMB data beyond WMAP also leads to a noticeable reduction in the preferred value of $\omega_{\rm b}$ and a corresponding increase in $\omega_{\rm dm}$.

To summarize, we find that there is evidence for $n_{\rm run} < 0$ in a limited class of models, but within the general ΛCDM model with 12 parameters the evidence is much weaker. Standard models of inflation are generally incompatible with such large negative values of $n_{\rm run}$, but the data appears to point in that direction, although not totally conclusively. The inclusion of an external prior from 2dF appears to weaken the result by fixing $\Omega_{\rm m} \approx 0.3$ in conjunction with the CMB data. The measurement of $\Omega_{\rm m}h$ using the galaxy power spectrum is responsible for this shift. It is an interesting question as to how reliable this measurement is since a slight shift in the results, a preference for $\Omega_{\rm m}h \approx 0.17$ rather than $\Omega_{\rm m}h \approx 0.21$ would bring their preferred value into line with that suggested by the CMB alone and would uphold the possibility of $n_{\rm run} < 0$. Since none of the galaxy redshift surveys have conclusively observed the turnover in the power spectrum on which this determination of $\Omega_{\rm m}h$ is based we assert that there is still room for some doubt. We have also investigated the possible systematic effects which could weaken our result. We believe that the assumptions behind the power spectrum measurements presented in Dickinson et al. (2004) are the best available using the observations which we have made and the other information from the literature we have used. For sure, we have shown that measurements of the CMB power spectrum beyond $\ell = 1000$ can have an impact on the estimation of cosmological parameters and that future measurements in this region by the VSA, the PLANCK satellite and others will enable us in the future to make more definitive statements.

ACKNOWLEDGEMENTS

We acknowledge S. Allen for permission to use his XLF probability curves, and H. Hoekstra for providing probability curves for cosmic shear. JAR-M acknowledges the hospitality of the IAC during several visits, and the financial support provided through the European Community's Human Potential Programme under contract HPRN-CT-2002-00124, CMBNET. KL, RS, CD acknowledge support by PPARC studentships. YAH is supported by the Space Research Institute of KACST. AS acknowledges the support of St. Johns College Cambridge. RAB thanks C. Contaldi and J. Weller for helpful comments and suggestions, and acknowledges the use of the COSMOS supercomputer based at DAMTP, Cambridge.

REFERENCES

Ahmad Q.R. et al., 2002, Phys. Rev. Lett. 89, 011301
Allen S., Schmidt R.W., Fabian A.C., 2002, MNRAS, 334, L11
Allen S., Schmidt R.W., Fabian A.C., Ebeling H., 2003a, MNRAS, 342, 287
Allen, S. W., Schmidt, R. W., & Bridle, S. L., 2003b, MNRAS, 346, 596
Allison W. W. M. et al., 1999, Phys. Lett. B449, 137
Ambrosio M. et al, 2000, Phys. Lett. B478, 5
Barger V., Lee H., Marfarti, 2003, Phys. Lett. B565, 33
Barriga J., Gaztanga E., Santos M.G, Sarkar S., 2001, MNRAS, 324, 977
Bennett C.L. et al., 1996, ApJ, 464, L1
Bennett C.L. et al., 2003, ApJS, 148, 1
Bridle S.L., Lewis A.W., Weller J., Efstathiou G., 2003, MNRAS, 342, L72
Burles S., Nollett K.M., Turner M.S., 2001, ApJ, 552, L1
Colless M. et al, 2001, MNRAS, 328, 1039
Dickinson C. et al., 2004, MNRAS, submitted
Efstathiou G., Bond J.R., 1999, MNRAS, 304, 75
Efstathiou G. et al., 2002, MNRAS, 330, L29
Efstathiou G. et al., 2003, astro-ph/0310207
Freedman W.L. et al., 2001, ApJ, 553, 47
Fukuda Y. et al. 1998 Phys. Rev. Lett 81, 1562
Fukuda Y. et al. 2002 Phys. Lett. B539, 179
Grainge K.J.B. et al., 2003, MNRAS, 341, L23
Halverson N.W. et al., 2002, ApJ, 568, 38
Hanany S. et al., 2002, ApJ, 545, L5
Hinshaw G. et al, 2003, ApJS, 148, 135
Hoekstra H., Yee H.K.C., Gladders M.D., 2002, ApJ, 577, 595
Kinney W.H., Kolb E.W., Melchiorri A, Riotto A., 2003, hep-ph/0305130
Kogut A. et al., 2003, ApJS, 148, 161
Kuo C.L. et al., 2004, ApJ, 600, 32
Leach S., Liddle A.R., 2003, astro-ph/0306305
Lewis A.L., Bridle S.L., 2002, PRD, 66, 103511
Mason B.S. et al., 1999, AJ, 118, 2908
Mason B.S. et al., 2003, ApJ, 591, 540
Mandelbaum R., McDonald P., Seljak U., Cen R., 2003, MNRAS, 344, 776
Netterfield C.B. et al., 2002, ApJ, 571, 604
Pearson T.J. et al., 2003, ApJ, 591, 556
Peiris H.V. et al., 2003, ApJS, 148, 213
Percival W.J. et al., 2001, MNRAS, 327, 1297
Percival W.J. et al., 2002, MNRAS, 337, 1068
Perlmutter S. et al., 1999, ApJ, 517, 565
Reiss A. et al., 1998, AJ, 116, 1009
Rubiño-Martin J.A. et al., 2003, MNRAS, 341, 1084
Seljak U., McDonald P., Makarov A., 2003, MNRAS, 342, L79
Scott P.F. et al., 2003, MNRAS, 341, 1076
Slosar A. et al., 2003, MNRAS, 341, L29
Smoot G.F. et al. 1992, ApJ, 396, L1
Spergel D.N. et al., ApJS , 2003, 148, 175
Tegmark M. et al., 2003, PRD, submitted (astro-ph/0310723)
Toffolatti L. et al., 1998, MNRAS, 297, 117
Verde L. et al., 2003, ApJS, 148, 195

This paper has been typeset from a TEX/ LATEX file prepared by the author.